THE AMERICAN SOCIETY OF MECHANICAL ENGINEERS
345 E. 47th St., New York, N.Y. 10017

96-GT-368

A VISCOPLASTIC CONSTITUTIVE THEORY FOR MONOLITHIC CERAMICS - I

Lesley A. Janosik
NASA Lewis Research Center
Cleveland, Ohio 44135

Stephen F. Duffy, PhD, PE
Cleveland State University
Cleveland, Ohio 44115

ABSTRACT

This paper, which is the first of two in a series, provides an overview of a viscoplastic constitutive model that accounts for time-dependent material deformation (e.g., creep, stress relaxation, etc.) in monolithic ceramics. Using continuum principles of engineering mechanics the complete theory is derived from a scalar dissipative potential function first proposed by Robinson (1978), and later utilized by Duffy (1988). Derivations based on a flow potential function provide an assurance that the inelastic boundary value problem is well posed, and solutions obtained are unique. The specific formulation used here for the threshold function (a component of the flow potential function) was originally proposed by Willam and Warnke (1975) in order to formulate constitutive equations for time-independent classical plasticity behavior observed in cement and unreinforced concrete. Here constitutive equations formulated for the flow law (strain rate) and evolutionary law employ stress invariants to define the functional dependence on the Cauchy stress and a tensorial state variable. This particular formulation of the viscoplastic model exhibits a sensitivity to hydrostatic stress, and allows different behavior in tension and compression.

NOMENCLATURE

a_{ij}	deviatoric component of the state variable tensor
B	constant (in general polynomial form of F)
C	coefficient used to simplify expressions for flow and evolutionary laws
F	Bingham-Prager threshold function
G	scalar state function
H	hardening constant
h	scalar hardening function dependent on the inelastic state variable
I_1, J_2, J_3	invariants associated with the Willam-Warnke threshold function F
$\mathfrak{I}_1, \mathfrak{J}_2, \mathfrak{J}_3$	invariants associated with the scalar function G
K	octahedral threshold shear stress
m, n	unitless exponents
R	recovery constant
r	position vector in Π-plane representing deviatoric component of a stress state
S_{ij}	deviatoric component of applied stress tensor
u, v	component of position vector r
Y	normalized threshold stress
α_{ij}	internal state variable tensor
$\dot{\alpha}_{ij}$	state variable evolutionary law
δ_{ij}	Kronecker delta
$\dot{\varepsilon}_{ij}$	flow law (inelastic strain rate)
η_{ij}	effective stress tensor
λ	scalar function in general polynomial form of F; dependent on J_3 through the angle of similitude θ
μ	viscosity constant
Π	plane perpendicular to the hydrostatic stress line in the Haigh-Westergaard stress space (i.e., the Π-plane)
π	3.14159 ···
ρ	Willam-Warnke hydrostatic threshold parameter
Σ_{ij}	effective deviatoric stress tensor
σ	threshold stress
σ_{ij}	applied Cauchy stress tensor
θ	angle of similitude measured in the Π-plane
Ω	scalar dissipative potential function

Presented at the International Gas Turbine and Aeroengine Congress & Exhibition
Birmingham, UK — June 10-13, 1996
This paper has been accepted for publication in the Transactions of the ASME
Discussion of it will be accepted at ASME Headquarters until September 30, 1996

Subscripts:

bc	equal biaxial compressive
c	compressive
i, j, k	tensorial components
m, n	tensorial components
q, u, v	tensorial components
t	tensile

Overstrike Characters:

~	denotes parameters associated with scalar function F
^	denotes parameters associated with scalar function G
·	rate

INTRODUCTION

With increasing use of ceramic materials in high temperature applications, the need arises to accurately predict thermomechanical behavior. This paper will focus on inelastic deformation behavior associated with these service conditions. A number of constitutive theories for materials that exhibit sensitivity to the hydrostatic component of stress have been proposed that characterize deformation using time-independent classical plasticity as a foundation. Corapcioglu and Uz (1978) reviewed several of these theories by focusing on the proposed form of the individual yield function. The review includes the works of Kuhn and Downey (1971), Shima and Oyane (1976) and Green (1972). Not included is the work by Gurson (1977) who not only developed a yield criteria and flow rule, but also discussed the role of void nucleation. Subsequent work by Mear and Hutchinson (1985) extended Gurson's work to include kinematic hardening of the yield surfaces. Although the previously mentioned theories admit a dependence on the hydrostatic component of stress, none of these theories allow different behavior in tension and compression. Willam and Warnke (1975) proposed a yield criterion for concrete that admits a dependence on the hydrostatic component of stress and explicitly allows different material responses in tension and compression. Several formulations of their model exist, i.e., a three-parameter formulation and a five-parameter formulation. For simplicity the work presented here builds on the three-parameter formulation.

The aforementioned theories are somewhat lacking in that they are unable to capture creep, relaxation and rate-sensitive phenomena exhibited by ceramic materials at high temperature. A noted exception is the recent work by Ding et al. (1994), as well as the work by White and Hazime (1995). Another exception is an article by Liu et al. (1995) which is an extension of the work presented by Ding and coworkers. As these authors point out, when subjected to elevated service temperatures, ceramic materials exhibit complex thermo-mechanical behavior that is inherently time dependent, and hereditary in the sense that current behavior depends not only on current conditions, but also on thermo-mechanical history. This paper presents the formulation of a macroscopic continuum theory that captures these time dependent phenomena. Specifically, the overview contained in this paper focuses on the complete multiaxial derivation of the constitutive model, and examines the attending geometrical implications when the Willam-Warnke (1975) yield function is utilized as a scalar threshold function. A second article, which will appear shortly, examines specific time-dependent stress-strain behavior that can be modeled with the constitutive relationship presented in this article. No attempt is made here to assess the accuracy of the model in comparison to experiment. A quantitative assessment is reserved for a later date, after the material constants have been suitably characterized for a specific ceramic material. The quantitative assessment could easily dovetail with the nascent efforts of White and coworkers.

FLOW POTENTIAL

Early work in the field of metal plasticity indicated that inelastic deformations are essentially unaffected by hydrostatic stress. This is not the case for ceramic based material systems, unless the ceramic is fully dense. The theory presented here allows for fully dense material behavior as a limiting case. In addition, as Chuang and Duffy (1994) point out, ceramic materials exhibit different time-dependent behavior in tension and compression. Thus inelastic deformation models for ceramics must be constructed in a fashion that admits sensitivity to hydrostatic stress and differing behavior in tension and compression. This will be accomplished here by developing an extension of a J_2 model first proposed by Robinson (1975) and later extended to sintered powder metals by Duffy (1988). Although the viscoplastic model presented by Duffy (1988) admitted a sensitivity to hydrostatic stress, it did not allow for different material behavior in tension and compression.

The complete theory is derivable from a scalar dissipative potential function identified here as Ω. Under isothermal conditions this function is dependent upon the applied stress (σ_{ij}) and internal state variable (α_{ij}), i.e.,

$$\Omega = \Omega\left(\sigma_{ij}\ \alpha_{ij}\right) \tag{1}$$

The stress dependence for a J_2 plasticity model or a J_2 viscoplasticity model is usually stipulated in terms of the deviatoric components of the applied stress, i.e.,

$$S_{ij} = \sigma_{ij} - (1/3)\sigma_{kk}\,\delta_{ij} \tag{2}$$

and a deviatoric state variable

$$a_{ij} = \alpha_{ij} - (1/3)\alpha_{kk}\,\delta_{ij} \tag{3}$$

For the viscoplasticity model presented here these deviatoric tensors are incorporated along with the effective stress

$$\eta_{ij} = \sigma_{ij} - \alpha_{ij} \tag{4}$$

and an effective deviatoric stress, identified as

$$\Sigma_{ij} = S_{ij} - a_{ij} \tag{5}$$

Both tensors, i.e., η_{ij} and Σ_{ij}, are utilized for notational convenience.

The potential nature of Ω is exhibited by the manner in which the flow and evolutionary laws are derived. The flow law is derived from Ω by taking the partial derivative with respect to the applied stress, i.e.,

$$\dot{\varepsilon}_{ij} = \frac{\partial \Omega}{\partial \sigma_{ij}} \tag{6}$$

The adoption of a flow potential and the concept of normality, as expressed in equation (6), were introduced by Rice (1970). In his work the above relationship was established using thermodynamic arguments. The authors wish to point out that equation (6) holds for each individual inelastic state.

The evolutionary law is similarly derived from the flow potential. The rate of change of the internal stress is expressed as

$$\dot{\alpha}_{ij} = -h\,\frac{\partial \Omega}{\partial \alpha_{ij}} \tag{7}$$

where h is a scalar function of the inelastic state variable (i.e., the internal stress) only. Using arguments similar to Rice's, Ponter and Leckie (1976) have demonstrated the appropriateness of this type of evolutionary law.

To give the flow potential a specific form, the following integral format proposed by Robinson (1978) is adopted

$$\Omega = K^2\left[\left(\frac{1}{2\mu}\right)\int F^n\,dF + \left(\frac{R}{H}\right)\int G^m\,dG\right] \tag{8}$$

where μ, R, H, and K are material constants. In this formulation μ is a viscosity constant, H is a hardening constant, n and m are unitless exponents, and R is associated with recovery. The octahedral threshold shear stress K appearing in equation (8) is generally considered a scalar state variable which accounts for isotropic hardening (or softening). However, since isotropic hardening is often negligible at high homologous temperatures ($\geq$ 0.5), to a first approximation K is taken to be a constant for metals. This assumption will be adopted in the present work regarding ceramic materials. The reader is directed to the work by Janosik (1996) for specific details regarding the experimental test matrix needed to characterize these parameters.

Several of the quantities identified as material constants in the theory are strongly temperature dependent in a non-isothermal environment. However, for simplicity, the present work is restricted to isothermal conditions. A paper by Robinson and Swindeman (1982) provides the approach by which an extension can be made to nonisothermal conditions. The present article concentrates on representing the complexities associated with establishing an inelastic constitutive model that will satisfy the assumptions stipulated herein for ceramic materials.

The dependence upon the effective stress Σ_{ij} and the deviatoric internal stress a_{ij} are introduced through the scalar functions

$$F = F\left(\Sigma_{ij}, \eta_{ij}\right) \tag{9}$$

and

$$G = G\left(a_{ij}, \alpha_{ij}\right) \tag{10}$$

Inclusion of η_{ij} and α_{ij} will account for sensitivity to hydrostatic stress. The concept of a threshold function was introduced by Bingham (1922) and later generalized by Hohenemser and Prager (1932). Correspondingly, F will be referred to as a Bingham-Prager threshold function. Inelastic deformation occurs only for those stress states where

$$F\left(\Sigma_{ij}, \eta_{ij}\right) > 0 \tag{11}$$

For frame indifference, the scalar functions F and G (and hence Ω) must be form invariant under all proper orthogonal transformations. This condition is ensured if the functions depend only on the principal invariants of Σ_{ij}, a_{ij}, η_{ij}, and α_{ij}, that is

$$F = F\left(\tilde{I}_1, \tilde{J}_2, \tilde{J}_3\right) \tag{12}$$

and

$$G = G\left(\mathcal{J}_1, \mathcal{J}_2, \mathcal{J}_3\right) \tag{13}$$

where

$$\tilde{I}_1 = \eta_{ii} \tag{14}$$

$$\tilde{J}_2 = \left(\frac{1}{2}\right) \Sigma_{ij}\, \Sigma_{ij} \tag{15}$$

$$\tilde{J}_3 = \left(\frac{1}{3}\right) \Sigma_{ij}\, \Sigma_{jk}\, \Sigma_{ki} \tag{16}$$

and

$$\mathcal{J}_1 = \alpha_{ii} \tag{17}$$

$$\mathcal{J}_2 = \left(\frac{1}{2}\right) \alpha_{ij}\, \alpha_{ij} \tag{18}$$

$$\mathcal{J}_3 = \left(\frac{1}{3}\right) \alpha_{ij}\, \alpha_{jk}\, \alpha_{ki} \tag{19}$$

These scalar quantities are elements of what is known in invariant theory as an integrity basis for the functions F and G.

A three parameter flow criterion proposed by Willam and Warnke (1975) will serve as the Bingham-Prager threshold function, F. The Willam-Warnke criterion uses the previously mentioned stress invariants to define the functional dependence on the Cauchy stress (σ_{ij}) and internal state variable (α_{ij}). In general, this flow criterion can be constructed from the following general polynomial

$$F = \lambda\left(\frac{\sqrt{\tilde{J}_2}}{\sigma_c}\right) + B\left(\frac{\tilde{I}_1}{\sigma_c}\right) - 1 \tag{20}$$

where σ_c is the uniaxial threshold flow stress in compression and B is a constant determined by considering homogeneously stressed elements in the virgin inelastic state, i.e.,

$$\alpha_{ij} = 0 \tag{21}$$

Note that a threshold flow stress is similar in nature to a yield stress in classical plasticity. In addition, λ is a function dependent on the invariant $\mathcal{J}_3$ and other threshold stress parameters that are defined momentarily. The specific details in deriving the final form of the function F can be found in Willam and Warnke (1975), and this final formulation is stated here as

$$F\left(\tilde{I}_1, \tilde{J}_2, \tilde{J}_3\right) = \frac{1}{\sigma_c}\left[\frac{1}{r(\tilde{\theta})}\right]\left[\frac{2\tilde{J}_2}{5}\right]^{1/2} + \frac{\tilde{I}_1}{3\rho\sigma_c} - 1 \tag{22}$$

for brevity. The function F is implicitly dependent on $\mathcal{J}_3$ through the function r which is characterized in the next section. This function is dependent on the angle of similitude $\tilde{\theta}$ which is defined by the expression

$$\cos\left(3\tilde{\theta}\right) = \frac{\left(3\sqrt{3}\right)\tilde{J}_3}{2\left(\tilde{J}_2\right)^{3/2}} \tag{23}$$

The invariant $\tilde{I}_1$ in equation (22) admits a sensitivity to hydrostatic stress. The invariant $\tilde{J}_3$ in equation (23) accounts for different behavior in tension and compression, since this invariant changes sign when the direction of a stress component is reversed. The parameter ρ characterizes the tensile hydrostatic threshold flow stress. This parameter will also be considered in more detail in the next section.

A similar functional form is adopted for the scalar state function G, i.e.,

$$G\left(\mathcal{J}_1, \mathcal{J}_2, \mathcal{J}_3\right) = \frac{1}{\sigma_c}\frac{1}{r(\hat{\theta})}\left[\frac{2\mathcal{J}_2}{5}\right]^{1/2} + \frac{\mathcal{J}_1}{3\rho\sigma_c} \tag{24}$$

The function G stipulated in the expression above is implicitly dependent on $\mathcal{J}_3$ through a second angle of similitude, $\hat{\theta}$, which is defined by the expression

$$\cos\left(3\hat{\theta}\right) = \frac{\left(3\sqrt{3}\right)\mathcal{J}_3}{2\left(\mathcal{J}_2\right)^{3/2}} \tag{25}$$

This formulation assumes a threshold does not exist for the scalar function G, and follows the framework of previously proposed constitutive models based on Robinson's (1978) viscoplastic law.

THRESHOLD PARAMETERS

For the Willam-Warnke three parameter formulation the model parameters include σ_t, the tensile uniaxial threshold stress,

σ_c, the compressive uniaxial threshold stress, and σ_{bc}, the equal biaxial compressive threshold stress. The function $r(\theta)$ appearing in equation (22) and the function $r(\hat{\theta})$ appearing in equation (24) depend implicitly on these parameters. This is demonstrated later in this section.

To explore the nature of the potential function, level surfaces of Ω are projected onto various stress subspaces for the virgin inelastic state. Restricting our view to the virgin inelastic state implies surfaces of Ω=constant are also surfaces of F=constant. As noted previously, F plays the role of a Bingham-Prager threshold function. Since there are an infinite family of surfaces F=constant, each associated with a particular magnitude of the inelastic strain rate, we restrict the scope of this discussion to threshold surfaces to gain an understanding of the physical nature of the current model.

The parameters σ_t and σ_c are depicted in Figure 1 where a threshold surface ($F=0$) has been projected onto the σ_{11}-σ_{22} stress subspace. For illustration, a set of threshold flow stress values has been adopted that roughly corresponds to values anticipated for isotropic monolithic ceramics. Specifically, the compressive uniaxial threshold stress value is σ_c = 2.00 MPa. The tensile uniaxial threshold stress value is σ_t = 0.20 MPa, and the equal biaxial compressive threshold stress value is σ_{bc} = 2.32 MPa.

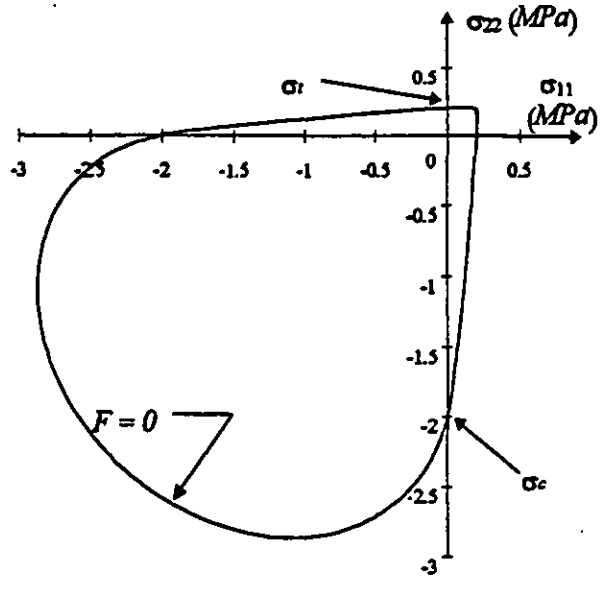

Figure 1 Threshold function projected onto the σ_{11} - σ_{22} stress plane.

Using these stress threshold values the flow function in Figure 1 defines a smooth flow surface for any combination of stresses. States of stress lying within the flow surface depicted in this figure represent elastic states of stress. Inelastic flow occurs when any load path reaches this surface, or other surfaces beyond (i.e., surfaces where $F>0$). It is readily discerned from this figure that the constitutive model allows different flow behavior in tension and compression.

The threshold parameter σ_{bc} can be seen when a cutting plane is passed through the flow surface ($F=0$) in the Haigh-Westergaard stress space. Specifically the cutting plane contains the hydrostatic stress line and it intersects the conic surface ($F=0$) along two lines (see Figure 2). By convention, these lines of intersection are termed meridians. The relative position of each meridian is defined by the angle of similitude $\bar{\theta}$ (which is depicted in Figure 3). For the tensile meridian $\bar{\theta}=0$, and for the compressive meridian $\bar{\theta}=\pi$. The tensile and compressive meridians, depicted in Figure 2, are linear for the three-parameter Willam-Warnke criterion. Meridians are nonlinear for the five-parameter formulation. In Figure 2 all three parameters, i.e., σ_t,

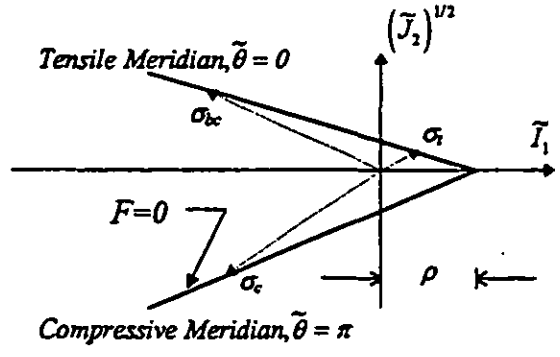

Figure 2 Threshold flow stresses defined by the tensile and compressive meridians

σ_c, and σ_{bc} are visible. These parameters are defined by the intersection of load paths with the flow surface. This characterization of the threshold flow stresses is described in detail in Palko (1992). Also note that this formulation of the Bingham-Prager flow function introduces a dependence on the hydrostatic component of the stress state. Combining views from Figures 2 and 3 in the Haigh-Westergaard stress space yields a flow surface in the shape of a pyramid with a triangular base. As a reference, typical J_2 plasticity models have yield surfaces that are right circular cylinders in the Haigh-Westergaard stress space.

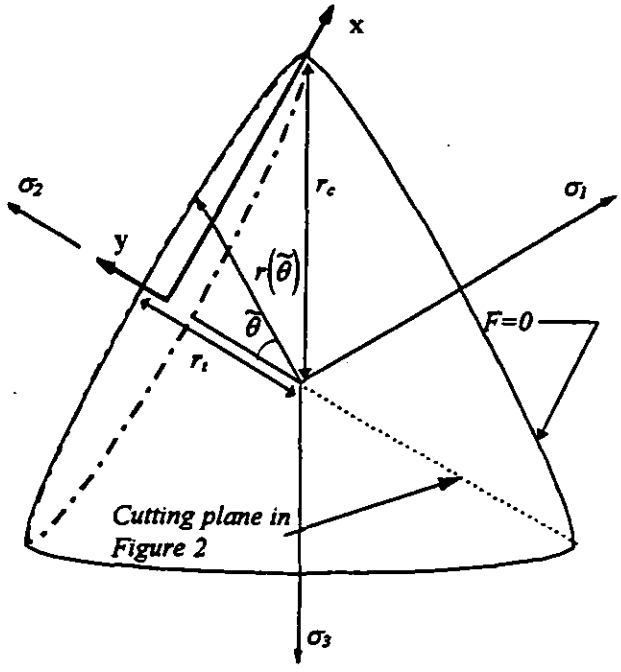

Figure 3 Flow surface projected onto the Π-plane in the Haigh-Westergaard stress space.

In lieu of the previously mentioned three threshold stress parameters, the threshold parameters

$$\rho = \frac{Y_{bc}\, Y_t}{Y_{bc} - Y_t} \tag{26}$$

$$r_t = \left(\frac{6}{5}\right)^{1/2} \frac{Y_{bc}\, Y_t}{2Y_{bc} + Y_t} \tag{27}$$

and

$$r_c = \left(\frac{6}{5}\right)^{1/2} \left[\frac{Y_{bc}\, Y_t}{3\, Y_{bc}\, Y_t + Y_{bc} - Y_t}\right] \tag{28}$$

are utilized in order to simplify the expression presented later for the function r. These alternative threshold stress parameters are dependent on the parameters σ_t, σ_c, and σ_{bc}. Specifically, the normalized threshold stresses

$$Y_t = \frac{\sigma_t}{\sigma_c} \tag{29}$$

and

$$Y_{bc} = \frac{\sigma_{bc}}{\sigma_c} \tag{30}$$

are introduced to simplify equations (26) through (28). Details of the derivations for the parameters appearing in equations (26) through (28) can be found in either Palko (1992) or Chen (1982).

The parameter ρ is depicted graphically in Figure 2. As noted earlier this parameter is the tensile threshold hydrostatic flow stress. Willam and Warnke postulated that a single sector ($-\pi/3 \le \theta \le \pi/3$) of the flow surface in the Π-plane could be represented as a segment of an ellipse. The major and minor axes of the ellipse are formulated as functions of the intercepts r_c and r_t (see Figure 3). The minor axis of the ellipse is assumed to coincide with a tensile axis. However, the center of the ellipse does not necessarily coincide with the hydrostatic axis, either for a material in the virgin state, or for a material that has been subjected to a service history. The reader should consult Palko (1992) for the complete derivation. With the function $r(\theta)$ defined the flow surface can be completely mapped in a Π-plane, as depicted in Figure 3.

For either $\bar{\theta}$ or $\hat{\theta}$ the function $r(\theta)$ is defined as

$$r(\theta) = \frac{u(\theta)}{v(\theta)} \tag{31}$$

where

$$\begin{aligned} u(\theta) = {} & 2r_c\left(r_c^2 - r_t^2\right)\cos(\theta) \\ & + r_c\left(2r_t - r_c\right)\left[4\left(r_c^2 - r_t^2\right)\cos^2(\theta)\right. \\ & \left. + 5r_t^2 - 4r_t r_c\right]^{1/2} \end{aligned} \tag{32}$$

and

$$v(\theta) = 4\left(r_c^2 - r_t^2\right)\cos^2(\theta) + \left(r_c - 2r_t\right)^2 \tag{33}$$

For the definitions expressed in equations (31) through (33)

$$-\frac{\pi}{3} \le \theta \le \frac{\pi}{3} \tag{34}$$

Physically, $r(\theta)$ represents the deviatoric component of a stress state, since this vector lies in the Π-plane. Note that equation (31) yields $r(\theta) = r_t$ for the special case of $\theta = 0$. Similarly, $r(\theta) = r_c$ for $\theta = \pi/3$.

FLOW SURFACES - INTERPRETATION

As in Robinson's original theory, the current model is closely tied to the concepts of a potential function and normality. It is this potential-normality structure that provides a consistent framework. According to the stability postulate of Drucker (1959), the concepts of normality and convexity are important requirements which must be imposed on the development of a flow or yield surface. Constitutive relationships developed on the basis of these requirements assure that the inelastic boundary-value problem is well posed, and solutions obtained are unique. Experimental work by Robinson and Ellis (1985) has demonstrated the validity of the potential-normality structure relative to an isotropic J_2 alloy (i.e., type 316 stainless steel). With this structure, the direction of the inelastic strain rate vector for each stress point on a given surface is directed normal to the flow surface F=constant (see Figure 4). Without experimental

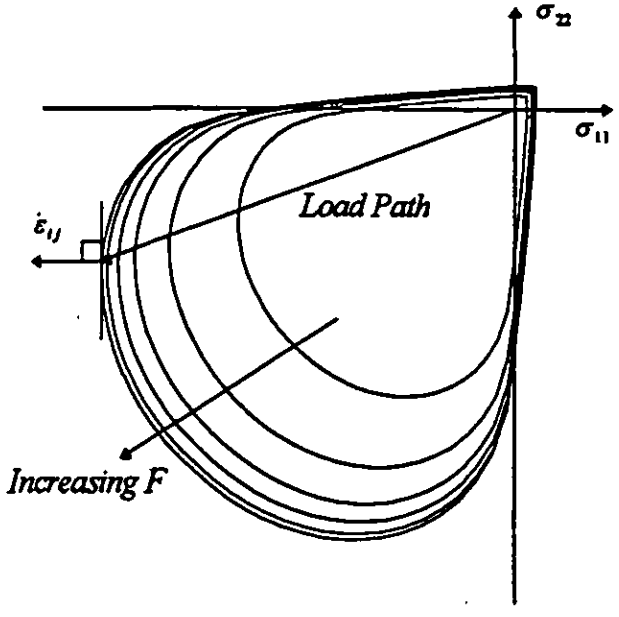

Figure 4 Flow surfaces associated with a monotonically increasing value of the flow function F.

evidence to the contrary, it is postulated that this structure is similarly valid for isotropic monolithic ceramic materials.

For constitutive models based on Robinson's (1978) original framework flow surfaces generated by non-zero values of F are associated with different inelastic strain rates. Figure 4 illustrates a typical family of level surfaces generated by monotonically increasing the magnitude of F (α_{ij}=0). The family is projected onto the σ_{11}-σ_{22} stress plane. Large values of F=constant correspond to flow surfaces that eventually cluster forming a limiting surface. This implies large changes in inelastic strain rate for only small stress changes, analogous to the yield condition of classical plasticity. This feature was pointed out originally by Rice (1970) for constitutive models based on equation (6).

The convexity of the proposed flow surface assures stable material behavior, i.e., positive dissipation of inelastic work, which is based on thermodynamic principles. The convexity requirement also implies that level surfaces of a function are closed surfaces, since an open region of the flow surface allows the existence of a load path along which failure will never occur.

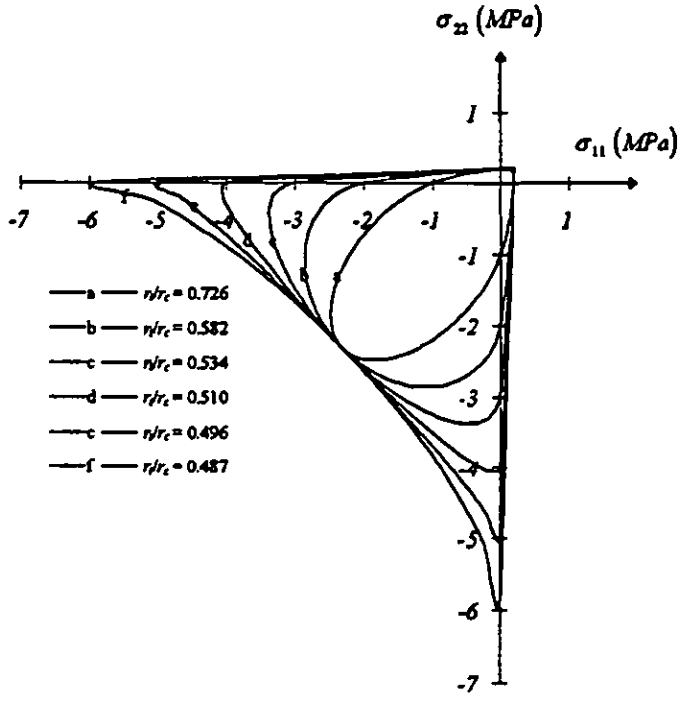

Figure 5 Flow surfaces as a function of the ratio r_i/r_c.

For the Willam-Warnke model, convexity is assured if the ratio of the intercepts in the Π-plane satisfies the condition $1.0 \geq r_i/r_c > 0.5$. The family of surfaces shown in Figure 5 illustrates the concept of convexity for surfaces having various r_i/r_c ratios. Here the values of the ratio vary from 0.726 to 0.487. Notice the surfaces identified as "e" and "f" violate the convexity condition.

Finally, the Willam-Warnke flow criterion (and the constitutive theory presented herein) degenerates to simpler models under special limiting conditions. For the case of $r_c = r_i = r_o$, where r_o is the same for any angle $\bar{\theta}$, the model degenerates to a two-parameter formulation, i.e., the Drucker-Prager flow criterion. When projected onto the σ_{11}-σ_{22} stress plane under these conditions, the flow surface depicted in Figure 1 degenerates to an ellipse (see Figure 6). Note that the major axis

of this ellipse is aligned with the bisector of the first and third quadrants, and the intercepts along the σ_{11} and σ_{22} axes represent uniaxial tensile and compressive threshold stresses that are not equal in magnitude, even though the flow surface degenerates to a circle in the Π-plane. The Drucker-Prager formulation yields

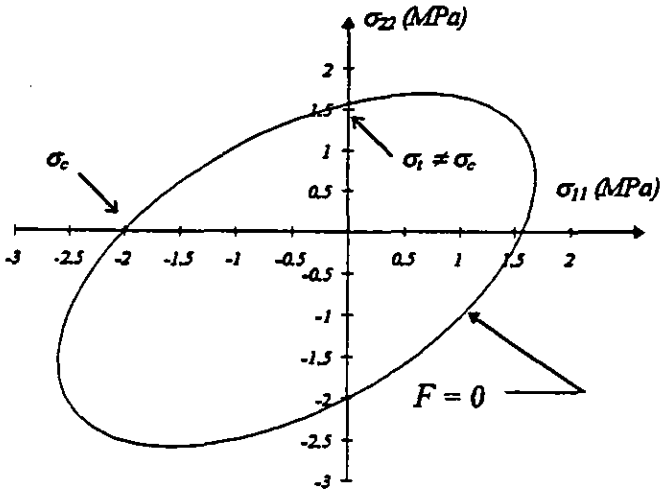

Figure 6 Flow surface for the Drucker-Prager formulation

different tensile and compressive threshold stresses because the formulation produces a right circular cone in the three-dimensional Haigh-Westergaard stress space. For the special case where $r_c = r_t = r_o$ and $\rho = \infty$, the Willam-Warnke model reduces to the single-parameter Von Mises criterion. For this case, the flow surface degenerates to a circle in the Π-plane (a right circular cylinder in the three-dimensional Haigh-Westergaard stress space) and an ellipse in σ_{11}–σ_{22} stress space, which is depicted in Figure 7.

STRESS-STRAIN RELATIONSHIP

Employing the chain rule for differentiation and taking the partial derivative of Ω with respect to σ_{ij}, as indicated in equation (6), yields

$$\dot{\varepsilon}_{ij} = \left(\frac{\partial \Omega}{\partial F}\right)\left[\frac{\partial F}{\partial \tilde{I}_1}\frac{\partial \tilde{I}_1}{\partial \eta_{kl}}\frac{\partial \eta_{kl}}{\partial \sigma_{ij}} + \frac{\partial F}{\partial \tilde{J}_2}\frac{\partial \tilde{J}_2}{\partial \Sigma_{uv}}\frac{\partial \Sigma_{uv}}{\partial S_{mn}}\frac{\partial S_{mn}}{\partial \sigma_{ij}} + \frac{\partial F}{\partial \tilde{J}_3}\frac{\partial \tilde{J}_3}{\partial \Sigma_{uv}}\frac{\partial \Sigma_{uv}}{\partial S_{mn}}\frac{\partial S_{mn}}{\partial \sigma_{ij}}\right] \quad (35)$$

where equation (8) has been utilized to define Ω.

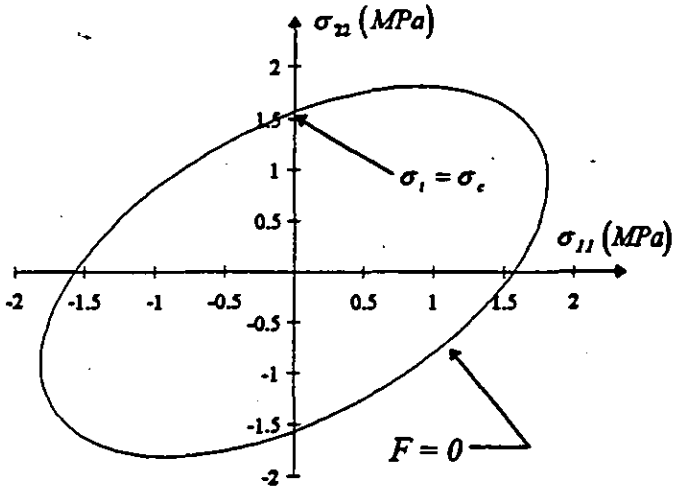

Figure 7 Flow surface for the Von Mises formulation

Evaluating the partial derivative terms in equation (35) yields the following expression for the flow law

$$\dot{\varepsilon}_{ij} = C_0\left[C_1\delta_{ij} + C_2\Sigma_{ij} + C_3\left(\Sigma_{jq}\Sigma_{qi} - \frac{2\tilde{J}_2\delta_{ij}}{3}\right)\right] \quad (36)$$

where the magnitudes of the coefficients C_0, C_1, C_2, and C_3 are dependent on the invariants defined in equations (14) through (16) (i.e., $\tilde{I}_1$, $\tilde{J}_2$, and $\tilde{J}_3$), the three threshold parameters (i.e., σ_t, σ_c, and σ_{bc}), and the flow potential parameters utilized in equation (8) (i.e., μ, K, and n). The first coefficient is defined by the expression

$$C_0 = \frac{K^2 F^n}{2\mu} \quad (37)$$

The remaining three coefficients are defined as

$$C_1 = \frac{1}{3\rho\sigma_c} \quad (38)$$

$$C_2 = \left[\frac{1}{2r(\tilde{\theta})\sigma_c}\right]\left[\frac{2}{5\tilde{J}_2}\right]^{1/2} - \frac{1}{\sigma_c}\left[\frac{1}{r(\tilde{\theta})}\right]^2\left[\frac{2\tilde{J}_2}{5}\right]^{1/2}\left[\frac{\partial r(\tilde{\theta})}{\partial \tilde{J}_2}\right] \quad (39)$$

and

$$C_3 = -\frac{1}{\sigma_e}\left[\frac{2\tilde{J}_2}{5}\right]^{1/2}\left[\frac{\partial r(\tilde{\theta})}{\partial \tilde{J}_3}\right]\left[\frac{1}{r(\tilde{\theta})}\right]^2 \quad (40)$$

Note that the partial derivatives of $r(\tilde{\theta})$ appearing in equations (39) and (40) are defined as

$$\frac{\partial r(\tilde{\theta})}{\partial \tilde{J}_2} = \left\{\frac{1}{v(\tilde{\theta})}\left[\frac{du(\tilde{\theta})}{d\tilde{\theta}}\right] - \frac{u(\tilde{\theta})}{v^2(\tilde{\theta})}\left[\frac{dv(\tilde{\theta})}{d\tilde{\theta}}\right]\right\}\left\{\frac{3\sqrt{3}\tilde{J}_3}{2\tilde{J}_2\left[4(\tilde{J}_2)^3 - 27(\tilde{J}_3)^2\right]^{1/2}}\right\} \quad (41)$$

and

$$\frac{\partial r(\tilde{\theta})}{\partial \tilde{J}_3} = -\left\{\frac{1}{v(\tilde{\theta})}\left[\frac{du(\tilde{\theta})}{d\theta}\right] - \frac{u(\tilde{\theta})}{v^2(\tilde{\theta})}\left[\frac{dv(\tilde{\theta})}{d\tilde{\theta}}\right]\right\}\left\{\frac{\sqrt{3}}{\left[4(\tilde{J}_2)^3 - 27(\tilde{J}_3)^2\right]^{1/2}}\right\} \quad (42)$$

where

$$\frac{du(\tilde{\theta})}{d\tilde{\theta}} = 2r_c\left(r_t^2 - r_c^2\right)\sin(\tilde{\theta}) + \frac{4r_c(2r_t - r_c)\left(r_t^2 - r_c^2\right)\sin(\tilde{\theta})\cos(\tilde{\theta})}{\left[4\left(r_c^2 - r_t^2\right)\cos^2(\tilde{\theta}) + 5r_t^2 - 4r_t r_c\right]^{1/2}} \quad (43)$$

and

$$\frac{dv(\tilde{\theta})}{d\tilde{\theta}} = 8\left(r_t^2 - r_c^2\right)\sin(\tilde{\theta})\cos(\tilde{\theta}) \quad (44)$$

Similarly, utilizing the chain rule for differentiation and taking the partial derivative of Ω with respect to the internal stress α_{ij} as indicated in equation (7) yields

$$\begin{aligned}\dot{\alpha}_{ij} &= -h\left(\frac{\partial\Omega}{\partial F}\frac{\partial F}{\partial \alpha_{ij}} + \frac{\partial\Omega}{\partial G}\frac{\partial G}{\partial \alpha_{ij}}\right) \\ &= -h\left\{\left(\frac{\partial\Omega}{\partial F}\right)\left[\frac{\partial F}{\partial \tilde{I}_1}\frac{\partial \tilde{I}_1}{\partial \eta_{kl}}\frac{\partial \eta_{kl}}{\partial \dot{\alpha}_{ij}} + \frac{\partial F}{\partial \tilde{J}_2}\frac{\partial \tilde{J}_2}{\partial \Sigma_{uv}}\frac{\partial \Sigma_{uv}}{\partial a_{mn}}\frac{\partial a_{mn}}{\partial \alpha_{ij}} + \frac{\partial F}{\partial \tilde{J}_3}\frac{\partial \tilde{J}_3}{\partial \Sigma_{uv}}\frac{\partial \Sigma_{uv}}{\partial a_{mn}}\frac{\partial a_{mn}}{\partial \alpha_{ij}}\right]\right. \\ &\quad \left. + \left(\frac{\partial\Omega}{\partial G}\right)\left[\frac{\partial G}{\partial J_1}\frac{\partial J_1}{\partial \alpha_{ij}} + \frac{\partial G}{\partial J_2}\frac{\partial J_2}{\partial a_{uv}}\frac{\partial a_{uv}}{\partial \alpha_{ij}} + \frac{\partial G}{\partial J_3}\frac{\partial J_3}{\partial a_{uv}}\frac{\partial a_{uv}}{\partial \alpha_{ij}}\right]\right\}\end{aligned} \quad (45)$$

Evaluating the partial derivative terms in equation (43) yields the following expression for the evolutionary law

$$\dot{\alpha}_{ij} = h\left\{\dot{\varepsilon}_{ij} - C_4\left[C_5\delta_{ij} + C_5 a_{ij} + C_6\left(a_{jq}a_{qi} - \frac{2}{3}\delta_{ij}\right)\right]\right\} \quad (46)$$

where $\dot{\varepsilon}_{ij}$ is given in equation (36). The magnitudes of the coefficients C_4, C_5, and C_6 are dependent on the invariants defined in equations (17) through (19) (i.e., J_1, J_2, and J_3), the three threshold parameters (i.e., σ_t, σ_c, and σ_{bc}), and the flow potential parameters utilized in equation (8) (i.e., R, H, K, and m). The first coefficient is defined by the expression

$$C_4 = \frac{K^1 R G^m}{H} \quad (47)$$

The remaining two coefficients are defined as

$$C_5 = \left[\frac{1}{2r(\hat{\theta})\sigma_c}\right]\left[\frac{2}{5 J_2}\right]^{1/2} - \frac{1}{\sigma_c}\left[\frac{1}{r(\hat{\theta})}\right]^2\left[\frac{2 J_2}{5}\right]^{1/2}\left[\frac{\partial r(\hat{\theta})}{\partial J_2}\right] \quad (48)$$

and

$$C_6 = -\frac{1}{\sigma_c}\left[\frac{2 J_2}{5}\right]^{1/2}\left[\frac{\partial r(\hat{\theta})}{\partial J_3}\right]\left[\frac{1}{r(\hat{\theta})}\right]^2 \quad (49)$$

Note that the partial derivatives of $r(\hat{\theta})$ appearing in equations (48) and (49) are defined as

$$\frac{\partial r(\hat{\theta})}{\partial J_2} = \left\{\frac{1}{v(\hat{\theta})}\left[\frac{du(\hat{\theta})}{d\hat{\theta}}\right] - \frac{u(\hat{\theta})}{v^2(\hat{\theta})}\left[\frac{dv(\hat{\theta})}{d\hat{\theta}}\right]\right\}\left\{\frac{3\sqrt{3} J_3}{2 J_2\left[4(J_2)^3 - 27(J_3)^2\right]^{1/2}}\right\} \quad (50)$$

and

$$\frac{\partial r(\hat{\theta})}{\partial J_3} = -\left\{\frac{1}{v(\hat{\theta})}\left[\frac{du(\hat{\theta})}{d\hat{\theta}}\right] - \frac{u(\hat{\theta})}{v^2(\hat{\theta})}\left[\frac{dv(\hat{\theta})}{d\hat{\theta}}\right]\right\}\left\{\frac{\sqrt{3}}{\left[4(J_2)^3 - 27(J_3)^2\right]^{1/2}}\right\} \quad (51)$$

Equations (36) and (46) constitute a multiaxial statement of a constitutive theory for isotropic materials. In the present and subsequent developments, it will serve as an inelastic deformation model for ceramic materials.

SUMMARY AND CONCLUSIONS

A multiaxial continuum theory was presented for predicting the inelastic response of isotropic monolithic ceramic materials. The viscoplastic constitutive model was derived from a single scalar dissipative function which has similar geometrical interpretations (e.g., convexity and normality) as the yield function encountered in classical plasticity. By adopting a flow potential to derive the theory, certain required continuum properties can be demonstrated, thereby ensuring that the resulting inelastic boundary value problem is well-posed, and solutions obtained are unique.

Constitutive equations for the flow law (strain rate) and evolutionary law are formulated based on a threshold function which exhibits a sensitivity to hydrostatic stress and allows different behavior in tension and compression. Further, inelastic deformation is treated as inherently time-dependent. A rate of inelastic strain is associated with every state of stress. As a result, creep, stress relaxation, and rate sensitivity are phenomena resulting from applied boundary conditions and are not treated separately in an ad hoc fashion.

The overview presented in this paper has provided a qualitative assessment of the capabilities of this viscoplastic model in capturing the complex thermomechanical behavior exhibited by ceramic materials at elevated service temperatures. Incorporating this model into a non-linear finite element code would provide industry the means to numerically simulate the inherently time-dependent and hereditary phenomena exhibited by these materials in service.

REFERENCES

Bingham, E.C., 1922, *Fluidity and Plasticity*, McGraw-Hill, New York.

Chen, W.F., 1982, *Plasticity in Reinforced Concrete*, McGraw-Hill, New York.

Chuang, T.-J., and Duffy, S.F., 1994, "A Methodology to Predict Creep Life for Advanced Ceramics Using Continuum Damage Mechanics," *Life Prediction Methodologies and Data for Ceramic Materials, ASTM STP 1201*, C.R. Brinkman and S.F. Duffy, Eds., American Society for Testing and Materials, Philadelphia, pp. 207-227.

Corapcioglu, Y., and Uz, T., 1978, "Constitutive Equations for Plastic Deformation of Porous Materials," *Powder Technology*, Vol. 21, pp. 269-274.

Ding, J.-L., Liu, K.C., and Brinkman, C.R., 1994, "A Comparative Study of Existing and Newly Proposed Models for Creep Deformation and Life Prediction of Si3N4," in *Life Prediction Methodologies and Data for Ceramic Materials, ASTM STP 1201*, C.R. Brinkman and S.F. Duffy, Eds., American Society for Testing and Materials, Philadelphia, pp. 62-83.

Drucker, D.C., 1959, "A Definition of Stable Inelastic Material", *Journal of Applied Mechanics*, Vol. 26; *ASME Transactions*, Vol. 81, pp. 101-106.

Duffy, S.F., 1988, "A Unified Inelastic Constitutive Theory for Sintered Powder Metals," *Mechanics of Materials*, Vol. 7, pp. 245-254.

Green, R.J., 1972, "A Plasticity Theory for Porous Solids," *International Journal for Mechanical Sciences*, Vol. 14, pp. 215.

Gurson, A.L., 1977, "Continuum Theory of Ductile Rupture by Void Nucleation and Growth: Part I—Yield Criteria and Flow Rules for Porous Ductile Media," *Journal of Engineering Materials and Technology*, Vol. 99, pp. 2-15.

Hohenemser, K., and Prager, W., 1932, "Ueber die Ansaetze der Mechanik Isotroper Kontinua," *Zeit fuer angewandte Mathematik und Mechanik*, Vol. 12.

Janosik, L.A., 1996, "A Unified Viscoplastic Constitutive Theory for Monolithic Ceramics," Master's Thesis, Cleveland State University, Cleveland, OH.

Kuhn, H.A., and Downey, C.L., 1971, "Deformation Characteristics and Plasticity Theory of Sintered Powder Metals," *International Journal of Powder Metallurgy*, Vol. 7, pp. 15-25.

Liu, K.C., Brinkman, C.R., Ding, J.-L., and Liu, S., 1995, "Predictions of Tensile Behavior and Strengths of Si_3N_4 Ceramic at High Temperatures Based on a Viscoplastic Model," ASME Transactions, 95-GT-388.

Mear, M.E., and Hutchinson, J.W., 1985, "Influence of Yield Surface Curvature on Flow Localization in Dilatant Plasticity," *Mechanics of Materials*, Vol. 4, pp. 395-407.

Palko, J.L., 1992, "Interactive Reliability Model for Whisker-Toughened Ceramics," Master's Thesis, Cleveland State University, Cleveland, OH.

Ponter, A.R.S., and Leckie, F.A., 1976, "Constitutive Relationships for Time-Dependent Deformation of Metals," *ASME Journal of Engineering Materials and Technology*, Vol. 98.

Rice, J.R., 1970, "On the Structure of Stress-Strain Relations for Time-Dependent Plastic Deformation in Metals," *Journal of Applied Mechanics*, 37, 728.

Robinson, D.N., 1978, "A Unified Creep-Plasticity Model for Structural Metals at High Temperature," ORNL/TM 5969.

Robinson, D.N., and Ellis, J.R., 1985, "Experimental Determination of Flow Potential Surfaces supporting a Multiaxial Formulation of Viscoplasticity," *Proceedings, 5th International Seminar on Inelastic Analysis and Life Prediction in High Temperature Environments*, Paris, France.

Robinson, D.N., and Swindeman, R.W., 1982, "Unified Creep-Plasticity Constitutive Equations for 2-1/4 CR-1 Mo Steel at Elevated Temperature," ORNL/TM 8444.

Shima, S., and Oyane, M., 1976, "Plasticity Theory for Porous Metals," *International Journal of Mechanical Sciences*, Vol. 18, pp. 285-

White, C.S., and Hazime, R.M., 1995, "Internal Variable Modeling of the Creep of Monolithic Ceramics," Proceedings of the 11th Biennial Conference on Reliability, Stress Analysis, and Failure Prevention, O. Jadaan, ed., The American Society of Mechanical Engineers, Philadelphia.

Willam, K.J., and Warnke, E.P., 1975, "Constitutive Model for the Triaxial Behaviour of Concrete, *Int. Assoc. Bridge Struct. Eng. Proc.*, Vol. 19, pp. 1-30.